

DUAL MESSAGE PASSING NEURAL NETWORK FOR MOLECULAR PROPERTY PREDICTION

A PREPRINT

Hehuan Ma

University of Texas at Arlington
Arlington, TX 76019
hehuan.ma@mavs.uta.edu

Yu Rong

Tencent AI Lab
Shenzhen, China 518057
yu.rong@hotmail.com

Wenbing Huang

Department of Computer Science and Technology
Tsinghua University
Beijing, China
hwenbing@126.com

Tingyang Xu

Tencent AI Lab
Shenzhen, China 518057
tingyangxu@tencent.com

Weiyang Xie

Tencent AI Lab
Shenzhen, China 518057
weiyangxie@tencent.com

Geyan Ye

Tencent AI Lab
Shenzhen, China 518057
blazerye@tencent.com

Junzhou Huang*

University of Texas at Arlington
Arlington, TX 76019
jzhuang@uta.edu

April 15, 2022

ABSTRACT

The crux of molecular property prediction is to conduct meaningful and informative representations of molecules. One promising way of doing this is exploiting the molecular graph structure, which leads to several graph-based deep learning models, such as Graph Neural Networks (GNN), Message Passing Networks (MPN), etc. However, current deep graph learning models generally focus on either node embedding or edge embedding. Since both atoms and chemical bonds play important roles in chemical reactions and reflect the property of molecules, existing methods fail to exploit both node(atom) and edge(bond) features simultaneously to make property prediction. In this paper, we propose **Dual Message Passing Neural Network (DualMPNN)**, a multi-view message passing architecture with a two-tier constraint, to make more accurate molecular property prediction. DualMPNN consists of two sub-models: one model as Node-MPN for atom-oriented modeling and the other as Edge-MPN for bond-oriented modeling. We design a shared self-attentive readout and disagreement loss to stabilize the training process and enhance the interactions between two sub-models. On the other hand, the designed self-attentive readout also provides the interpretability for molecular property prediction, which is crucial for real applications like molecular design and drug discovery. Our extensive experimental evaluations demonstrate that DualMPNN achieves remarkably superior improvement over the state-of-the-art approaches on a variety of challenging benchmarks. Meanwhile, the visualization of the self-attention demonstrates how different atoms affect the prediction performance, which brings in the interpretability of deep learning models out of the black-box.

Keywords molecular property prediction · message passing neural network · graph neural network · graph classification

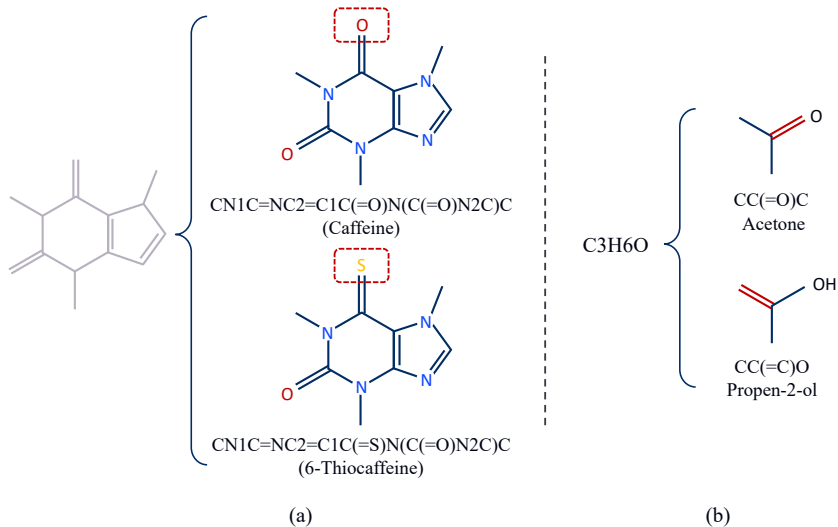


Figure 1: (a) Two molecules with same bonds, but different atoms. Noted, atom *O* and atom *S* are different. (b) Two molecules with same atoms, but different bonds.

1 Introduction

Molecular property prediction is a crucial and challenging task in chemical drug discovery area, since it helps to determine the functionality of new drugs. Many researches have been done for it over years. For example, design molecular fingerprint based on the radial group of the molecular structure, then use the converted fingerprint to implement property prediction [1]. Specifically, a particular property of a given molecule is identified by applying specific models. However, traditional molecular property prediction methods usually 1) require chemical experts to conduct professional experiments to validate the property label, 2) desire high R&D cost and massive time, and 3) ask for specialized model for different properties, which lacks universality [2, 3].

To date, Graph Neural Network (GNN) has gained more and more attention due to its capability of dealing with graph structured data. Certain successes have been achieved in many domains, such as social network analysis [4, 5], knowledge-graphs [6, 7], and recommendation systems [8, 9]. Molecular property prediction is also a promising application of GNN since a molecule could be represented as a graph structure by treating atoms as nodes, and bonds as edges. Compared with the other representations for molecules, such as SMILES[10], which represents molecules as sequences but losses structural information, graph representation of molecules can naturally reveal the information from molecular structure, including both the nodes (atoms) and edges (bonds). In this sense, a molecular property prediction is equivalent to a supervised graph classification problem (see, for example, toxicity prediction [11] and protein interface prediction [12]).

Despite the fruitful results obtained by GNN, there still remains two limitations for current GNN models when apply them to molecular property prediction: on the one side, 1) Most of the GNN models only focus on the embedding of nodes. It is truthful that nodes play an dominant role in many graph-based scenarios including social network, recommendation system, citation network, and so on. However, in some cases, nodes and edges play the equally important roles. For example, in a knowledge graph, a node represents an entity, and the edge holds the interact ontologies and semantics between linked nodes. Different edges that represent different relations hence may lead to the different answers. Especially, molecular property prediction also demands information from both atoms and bonds to generate precise graph embedding and make accurate prediction. Molecules with different atoms(nodes) but same bonds(edges) are distinct compounds with different properties and so as to different bonds(edges) but same atoms(nodes). As shown in Figure.1(a), equipped with same bonds, only one-atom difference make the two molecules distinct Octanol/Water Partition Coefficients. Caffeine is more hydrophilic while 6-Thiocaffeine is more lipophilic[13]. Similarly, with Fig.1(b), the molecular formulas of Acetone and Propen-2-ol are exactly the same, but the bond variance makes Acetone behave mild irritation to human eyes, nose, skin, etc. Accordingly, both nodes and edges are fairly essential for molecular property prediction. Therefore, *how to properly integrate both node and edge information in a single model* is the first challenging issue. On the other side, 2) the second limitation is the interpretability of the models. It is not doubted that the interpretability is very important for drug discovery. Even it is straightforward to feed the chemical data into the network and obtain a result, understanding how the underlying model work will also help crack the problem. Take molecular property prediction as an example, getting clear with how the model validate the property

will help people figure out the key components of determining certain properties[14]. The lack of interpretability is the main obstacle to adopt machine learning models into such areas. Consequently, *How to give the explanation of the prediction results* is the second challenging issue.

To address those challenges, we believe that a fresh perspective of viewing the graph from two aspects covering both nodes and edges would be more meaningful and precise. In this paper, we take Message Passing Neural Network (MPN) [15] as the backbone¹, and propose a new architecture: DualMPNN based on the popularity of multi-view learning, which considers the diversity of different aspects for one single target[16]. DualMPNN consists of two sub-models that generate the graph embedding vectors from node and edge, respectively. Therefore, it observes the target molecular graph from two diverse views, node-central and edge-central, simultaneously. Meanwhile, we design a shared self-attentive readout instead of a mean-pooling readout to produce the graph-level embedding from node embeddings. The shared self-attentive readout not only integrates the information from node and edge views but also brings the interpretability to DualMPNN. Furthermore, to stabilize the training of the dual architecture, we introduce a disagreement loss to restrain the difference of the predictions between two sub-models. Therefore, DualMPNN, as a multi-view based architecture, is more efficient than single-view learning with better generalization capacity. Comprehensive experiments on various kinds of benchmarks demonstrate the superiority of DualMPNN. Overall, the key contributions of the paper could be summarized as follows:

- We propose DualMPNN, a multi-view learning architecture to solve the molecular property prediction problem. To the best of our knowledge, DualMPNN is the first property prediction model that focuses on both node information and edge information in a unified way.
- We introduce the shared self-attentive readout to DualMPNN that brings the interpretability into the molecular property prediction models, which is essential for the real applications.
- Extensive experiments on 11 benchmark data sets validate the effectiveness of DualMPNN. Namely, the overall performance of DualMPNN achieves at least 2% improvement on classification benchmarks and 8.2% improvement on regression benchmarks compared with the state-of-the-art (SOTA) methods. Moreover, the cast studies on toxicity prediction datasets demonstrates the interpretability of DualMPNN on practical applications.

2 Preliminary

An essential preliminary is to represent a molecule to a graph representation, and extract the initial features. We view a molecule c as a graph $G_c = (\mathcal{V}, \mathcal{E})$, where $|\mathcal{V}| = p$ refers to a set of p nodes (atoms) in the molecule and $|\mathcal{E}| = q$ refers to a set of q edges (bonds) in the molecule satisfying $(v_i, v_j) \in \mathcal{E}$. We also denote \mathcal{N}_v as the neighborhood set of node v in the graph. Other than the graph structure, molecules also contains node and edge features. We denote the feature of node v as $\mathbf{x}_v \in \mathbb{R}^{d_n}$ and the feature of edge (v, k) as $\mathbf{e}_{vk} \in \mathbb{R}^{d_e}$ ². Note that d_n and d_e refer to the feature dimension of nodes and edges, respectively. One possible node features and edge features are the initial chemical relevant features such as atomic mass and bond type. Please refer to appendix for more detailed feature extraction process. We denote a property \mathbf{y} as the target of the predictive task. The values of \mathbf{y} are either binary values for classification tasks or real values for regression tasks because some properties of the molecules, such as the toxicity and the permeability[17, 18], are treated as labels while some properties, such as the atomization energy and the electronic spectra are treated as real values[19, 20].

Therefore, it is straightforward to formulate the molecular property prediction problem as:

Definition 2.1. Given a molecule c and its graph G_c , molecular property prediction aims to predict the property \mathbf{y}_c according to the graph representation ξ_c that is mapped from G_c .

3 Methodologies

In this section, we present the **Dual Message Passing Neural Network** (DualMPNN) for molecular property prediction. We first introduce an overall framework of DualMPNN. Then, we describe different components in detail.

3.1 Framework Overview

In order to find different appropriate and accurate representations of a molecule, we aim at obtaining sufficient information from the graph structure of the molecule, including both atoms features (node information) and bond

¹Here, the backbone can be any valid GNNs depending on the applications

²Without ambiguous, \mathbf{e}_{vk} can represent either the edge or the edge features.

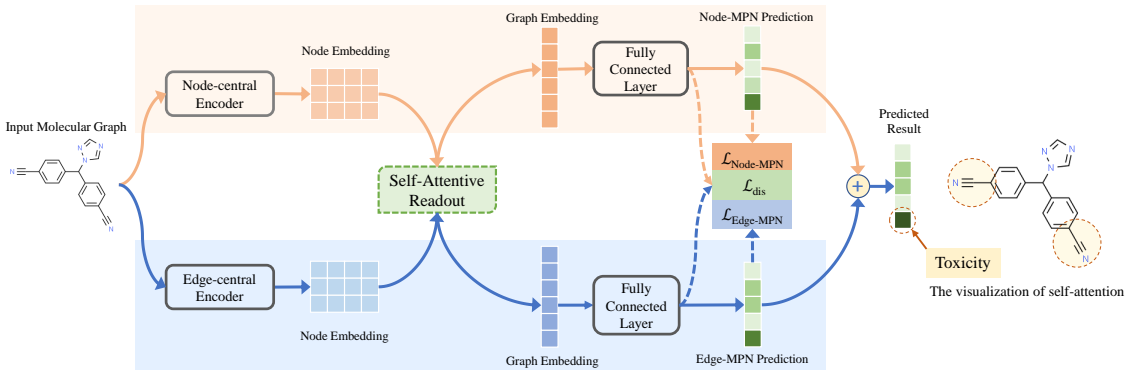


Figure 2: DualMPNN overview. DualMPNN takes the molecular graph as the input, then passes through two encoders to get two node embeddings from different perspectives. A shared self-attention readout learns the node importance and produce two graph embedding vectors accordingly. The graph embeddings is then fed into two distinct fully connected layer to implement the prediction tasks. The final prediction of DualMPNN is the simple ensemble of the predictions from two encoders. Furthermore, by visualizing the learned attentions over nodes, we can find the atoms/functional groups that are important for the predicted proprieties. For example, DualMPNN can identify the cyano groups in this compound contribute to the toxicity significantly.

features (edge information), since both of them are important for determining the molecular property. In this fashion, atom features and bond features should be considered equally important for constituting a molecular representation vector based on its graph structure.

As demonstrated in Figure 2, DualMPNN architecture contains two concurrent phases, **Node-central Encoder** and **Edge-central Encoder**, which output the node / edge embedding matrix from the graph topology as well as node / edge features. Here, we employ the message passing neural network[15], which has achieved remarkable success in modeling molecules, as the backbone to design **Node-central Encoder** and **Edge-central Encoder**, respectively.

Next, DualMPNN adopts an aggregation function to produce the graph embedding vector from node / edge embedding matrix. Other than the mean-pooling mechanisms used in [21], we propose to use the **self-attentive aggregation** to learn the different weights of each embedding to produce the graph embedding. Furthermore, we share the self-attentive aggregation layer between Node-central Encoder and Edge-central Encoder to reinforce the learning of node features and edge features, respectively.

After the self-attentive aggregation, DualMPNN feeds the graph embeddings from Node-central Encoder and Edge-central Encoder to two independent fully connected(FC) layers to fit a loss function depending on the concrete prediction task, respectively. To stabilize the training process of this dual architecture, we employ the **Disagreement Loss** to enforce the output of two fully connected layer similar with each other.

3.2 Node-central and Edge-central Encoders

In this section, we introduce the construction of Node-central and Edge-central Encoders in DualMPNN.

Message Passing Neural Network(MPN). The message passing neural network is originally proposed in [15], which can be viewed as the simulation of information diffusion in graphs. Specially, it aggregates and passes the features information of corresponding neighbor nodes to produce the new embeddings. Therefore, given a node v as an example, we can define the general form of feed-forward layer of MPN as follows:

$$\begin{aligned} \mathbf{m}'_v &= \text{AGG}_{u \in \mathcal{N}_v}(\mathcal{M}(\mathbf{h}_u, \boldsymbol{\mu}_{\text{att}})) \\ \mathbf{h}'_v &= \mathcal{U}(\mathbf{h}_v, \mathbf{m}'_v). \end{aligned} \quad (1)$$

where, \mathbf{h}'_v refers to the state vector of node v from the layer with $\mathbf{h}_u, u \in \mathcal{N}_v$ as the input embeddings; $\boldsymbol{\mu}_{\text{att}}$ represents the attached features of node v during aggregation; and \mathbf{m}'_v is the message vector for node v . From (1), MPN contains two phases: message passing and state update. In message passing phase, \mathcal{M} is a message update function to combine the information from \mathbf{h}_u and $\boldsymbol{\mu}_{\text{att}}$ and AGG is the message aggregation function to produce the messages \mathbf{m}'_v with the neighbor information. After that, the state update function \mathcal{U} is applied to produce the output embedding vector \mathbf{h}'_v with the input embedding of node v .

Taking MPN as the backbone, in the following, we define the Node-central and Edge-central Encoders, respectively.

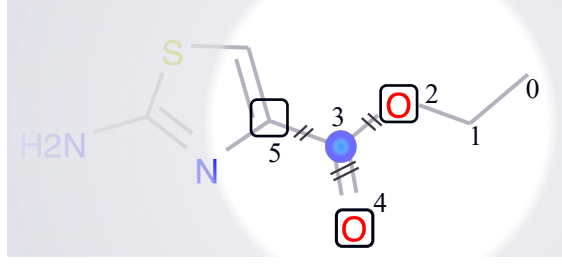


Figure 3: Node-MPN Model. For the node message construction, take node v_3 as an example. 1) neighbor node aggregation: aggregate the node features of its neighbor nodes v_2 , v_4 and v_5 ; 2) μ_{att} : get the initial edge features as the attached features from the connected edge e_{23} , e_{34} , and e_{35} ; 3) update the state of v_3 using (2).

3.2.1 Node-central Encoder.

It is straightforward to utilize MPN to formulate Node-central Encoder in DualMPNN. Specifically, we define Node-MPN as follows:

$$\begin{aligned} \mathbf{m}_v^{(l+1)} &= \sum_{u \in \mathcal{N}_v} \text{CONCAT}(\mathbf{h}_u^{(l)}, \mathbf{e}_{vu}), \\ \mathbf{h}_v^{(l+1)} &= \sigma(\mathbf{W}_{\text{node}} \mathbf{m}_v^{(l+1)} + \mathbf{h}_v^{(0)}), \end{aligned} \quad (2)$$

where $\mathbf{h}_v^{(0)} = \sigma(\mathbf{W}_{\text{nin}} \mathbf{x}_v)$ is the input state of Node-MPN, and $\mathbf{W}_{\text{nin}} \in \mathbb{R}^{d_{\text{hid}} \times d_n}$ is the input weight matrix with an input dimension, d_{hid} . In message passing phase, Node-MPN employs the summation (SUM) as the message aggregation function, and concatenation CONCAT as the message update function to generate the message vector $\mathbf{m}_v^{(l+1)}$. In state update phase, Node-MPN employs a linear transformation with activation function $\sigma(\mathbf{W}_{\text{node}} \mathbf{m}_v^{(l+1)} + \mathbf{h}_v^{(0)})$ as the state update function \mathcal{U} . Here $\mathbf{W}_{\text{node}} \in \mathbb{R}^{d_{\text{hid}} \times (d_n + d_{\text{hid}})}$ is the weight matrix and $\sigma(\cdot)$ is the activation function³.

The messaging passing process in Node-MPN contains L steps. At $l+1$ step, Node-MPN updates state of node v by aggregating the previous state of its neighbor node $u \in \mathcal{N}_v$ as well as the corresponding edge feature \mathbf{e}_{vu} to generates a new states of node v . \mathbf{W}_{node} is the model parameter shared in all steps. Figure 3 depicts an example of the message passing process in Node-MPN.

After L step message passing, we utilize an additional message passing step with different weight matrix $\mathbf{W}_{\text{nout}} \in \mathbb{R}^{d_{\text{out}} \times (d_n + d_{\text{hid}})}$ to produce the final node embedding:

$$\begin{aligned} \mathbf{m}_v^o &= \sum_{k \in \mathcal{N}_v} \text{CONCAT}(\mathbf{h}_k^{(L)}, \mathbf{x}_k) \\ \mathbf{h}_v^o &= \sigma(\mathbf{W}_{\text{nout}} \mathbf{m}_v^o). \end{aligned} \quad (3)$$

By adding this additional message passing process, we can introduce more parameters as well as the non-linearity to enhance the description power of Node-MPN. We denote $\mathbf{H}_n = [\mathbf{h}_1^o, \dots, \mathbf{h}_p^o] \in \mathbb{R}^{d_{\text{out}} \times p}$ as the output embeddings of Node-MPN. d_{out} is the dimension of output embedding.

3.2.2 Edge-central Encoder

In graph theory, the line graph $L(G)$ of graph G is the graph that represents the adjacencies between edges of G [22]. The line graph provides us a fresh perspective to understand the original graph, that is, the nodes can be viewed as the connections while edges can be viewed as entities. Therefore, it is possible to perform the message passing through nodes to imitate Node-MPN on $L(G)$ [21]. Namely, given an edge (v, w) , The Edge-based MPN (Edge-MPN) is formulated as:

$$\begin{aligned} \mathbf{m}_{vw}^{(l+1)} &= \sum_{u \in \mathcal{N}_v \setminus w} \text{CONCAT}(\mathbf{h}_{uv}^{(l)}, \mathbf{x}_u) \\ \mathbf{h}_{vw}^{(l+1)} &= \sigma(\mathbf{W}_{\text{edge}} \mathbf{m}_{vw}^{(l+1)} + \mathbf{h}_{vw}^{(0)}), \end{aligned} \quad (4)$$

where $\mathbf{h}_{vw}^{(0)} = \sigma(\mathbf{W}_{\text{ein}} \mathbf{e}_{vw})$ is the input state of Edge-MPN. $\mathbf{W}_{\text{ein}} \in \mathbb{R}^{d_{\text{hid}} \times d_e}$ is the input weight matrix. In (4), the state vector is defined on edge \mathbf{e}_{vw} . Meanwhile, we define the neighbor edge set of \mathbf{e}_{vw} by all edges connected to the

³Without any specification, we use ReLu as the activation function by default.

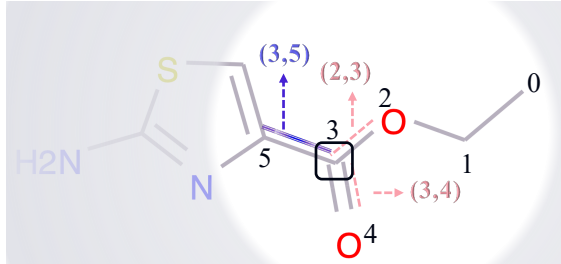


Figure 4: Edge-MPN Model. For the edge message construction, take edge e_{35} as an example. 1) neighbor edge aggregation: aggregate the edge features of its neighbor edges, edge e_{23} , edge e_{34} ; 2) μ_{att} : get the initial node information as the attached features from the endpoint node v_2 of edge e_{23} , node v_4 of e_{43} ; 3) updated the message of e_{35} using (4).

start node v except node w . The attached feature μ_{att} is the bond feature x_k . The message passing and state update phase is similar with Node-MPN. Edge-MPN also contains L steps. Figure 4 depicts an example of the message passing process in Edge-MPN.

After recurring L steps for the message passing, the output of Edge-MPN is the states for edges. In order to incorporate the shared-attentive readout to generate the graph embedding, one more round message passing on nodes is employed to transform edge-wise embedding to node-wise embedding, and generate the final node embedding: h_v^o :

$$\begin{aligned} m_v^o &= \sum_{k \in \mathcal{N}_v} \text{CONCAT}(h_{kv}^{(L)}, x_k) \\ h_v^o &= \sigma(W_{\text{eout}} m_v^o), \end{aligned} \quad (5)$$

where $W_{\text{eout}} \in \mathbb{R}^{d_{\text{out}} \times (d_n + d_{\text{hid}})}$ is the weight matrix. Therefore, the final output of Edge-MPN is represented as $H_e = [h_1^o, \dots, h_p^o] \in \mathbb{R}^{d_{\text{out}} \times p}$.

3.3 Readout for Graph-level Embedding

As discussed in Section 3.2, the outputs of Node-central and Edge-central Encoders are both depending on the node numbers. To obtain a fixed length graph representation, a readout transformation is needed to eliminate the obstacle of size variance and permutation variance. Here, we introduce two readout transformations to obtain the molecular representation:

Mean-Pooling Readout. A straightforward solution is to aggregate each node embedding in the graph by mean-pooling. For instance, given an output of Node-central Encoder $H_n \in \mathbb{R}^{d_{\text{out}} \times p}$, we produce the molecular representation by:

$$\xi_n = \frac{1}{p} \sum_{h_i^o \in H_n} h_i^o \quad (6)$$

One limitation of the mean pooling is, the average operation tends to produce the smooth outputs. Therefore, it diminishes the power of capturing important features in the graphs. This drawback is more apparent within larger graphs.

Self-Attentive Readout. To overcome the drawbacks of mean-pooling, we employ the self-attention mechanism, which is introduced in [4, 23], to learn the node importance and encode node embedding into a size-invariant graph embedding vector. Namely, given an output of Node-central Encoder $H_n \in \mathbb{R}^{d_{\text{out}} \times p}$, the self-attention S over nodes is defined as:

$$S = \text{softmax}(W_2 \tanh(W_1 H_n^T)), \quad (7)$$

where $W_1 \in \mathbb{R}^{d_{\text{attn}} \times p}$ and $W_2 \in \mathbb{R}^{r \times d_{\text{attn}}}$ are two weight matrices. In (7), W_1 is to linearly transform the atom embedding from p -dimensional space to a d_{attn} -dimensional space. The \tanh function is equipped for introducing nonlinearity. W_2 brings r different insights of node importance, then followed a softmax function to normalize the importance, which makes the summation of different importance views to 1. To enable the feature information extracted from Node-central and Edge-central Encoders binding and communicating during the dual training process, we share the attention parameter S between two sub-models.

According to the self-attention matrix S , we can obtain the **size invariant** and **node importance involved** graph embedding $\xi \in \mathbb{R}^{r \times d_{\text{out}}}$ as follows:

$$\xi_n = \text{Flatten}(S H_n) \quad (8)$$

The self-attention \mathbf{S} can be viewed as the importance of the nodes when generating the graph embedding. Therefore, in this end-to-end framework, we can utilize \mathbf{S} to indicate the contributions of the nodes for the downstream tasks. In the other words, this Self-Attentive Readout can bring the interpretability of DualMPNN.

3.4 The Loss of DualMPNN

After obtaining the graph embedding from Node-central and Edge-central Encoders, we feed ξ_n and ξ_e into two distinct fully connected neural networks to obtain the predictions of two encoders respectively. Formally, we formulate this molecular property prediction loss as follows:

$$\mathcal{L}_{\text{DualMPNN}} = \mathcal{L}_{\text{pred}} + \lambda \mathcal{L}_{\text{dis}}, \quad (9)$$

where $\mathcal{L}_{\text{pred}}$ is the supervised loss and \mathcal{L}_{dis} is the disagreement loss for two predictions. λ is a hyper-parameter indicating the coefficient of the disagreement loss.

The supervised loss. The supervised loss includes the prediction losses of two encoders. The concrete loss formulation depends on the task types, e.g., Cross-Entropy for classification and Mean Square Error for regression. Generally, given the molecular graph set $\mathcal{G} = \{G_i\}_{i=1}^K$ and corresponding labels $\mathcal{Y} = \{y_i\}_{i=1}^K$, we formulate this molecular property prediction loss as follows:

$$\mathcal{L}_{\text{pred}} = \sum_{G_i \in \mathcal{G}} (\mathcal{L}_{\text{Node-MPN}}(\mathbf{y}_i, \gamma_{n,i}) + \mathcal{L}_{\text{Edge-MPN}}(\mathbf{y}_i, \gamma_{e,i})), \quad (10)$$

where $\gamma_{*,i}$ is the output predictions produced by a fully connected neural network given graph embedding $\xi_{*,i}$, i.e., $\gamma_{*,i} = \text{ffn}(\xi_{*,i})$, $*$ = n, e.

The disagreement loss. Other than the supervised loss, another crucial loss is introduced to stabilize the dual architecture. The disagreement loss is responsible for restraining the two predictions from Node-central and Edge-central Encoders. From the multi-view learning perspective, the graph embeddings from two encoders can be viewed as the different aspects for one single target (the molecule)[16]. Therefore, no matter how the graph embedding is generated, the predictions of this single target ought to be the same. Hence, the disagreement loss is to minimize the difference between γ_{n,G_i} and γ_{e,G_i} . Here, we employ the Mean Square Error to measure the disagreement loss:

$$\mathcal{L}_{\text{dis}} = \sum_{G_i \in \mathcal{G}} |\gamma_{n,i} - \gamma_{e,i}|^2 \quad (11)$$

Overall, the shared self-attentive readout and the disagreement loss in the mixed loss function alleviate the node variant dependency, and reinforce the restriction during the training to promise the model converge to a stationary status.

4 Experiments

In this section, we first conduct the performance evaluation of DualMPNN with several state-of-the-arts baselines on both molecular property classification and regression tasks. Then we preform the ablation study on the variants of DualMPNN. At last, we conduct a case study to demonstrate the interpretability of DualMPNN.

4.1 Datasets

We conduct our experiments on 11 popular benchmark datasets on molecular property prediction, 6 of them are classification tasks and the others are regression tasks. Here are the detailed description of the datasets:

Molecular Classification.

- **BACE** dataset is collected for recording compounds which could act as the inhibitors of human β -secretase 1 (BACE-1) in the past few years [24].
- The Blood-brain barrier penetration (**BBBP**) dataset contains the records of whether a compound carries the permeability property of penetrating the blood-brain barrier [18].
- **Tox21** and **ToxCast** datasets include multiple toxicity labels over thousands of compounds by running high-throughput screening test on thousands of chemicals [17].
- **SIDER** documents marketed drug along with its adverse drug reactions, also known as the Side Effect Resource [25].

Table 1: Datasets Statistics, six datasets are used for classification, and five datasets are used for regression.

Task	Dataset	# Tasks	# Graphs	Metric
Classification	BACE	1	1513	AUC-ROC
	BBBP	1	2039	AUC-ROC
	Tox21	12	7831	AUC-ROC
	ToxCast	617	8574	AUC-ROC
	SIDER	27	1427	AUC-ROC
	ClinTox	2	1478	AUC-ROC
Regression	QM7	1	6830	MAE
	QM8	12	21786	MAE
	ESOL	1	1128	RMSE
	Lipophilicity	1	4200	RMSE
	FreeSolv	1	642	RMSE

- **ClinTox** dataset compares drugs approved through FDA and drugs eliminated due to the toxicity during clinical trials [26].

Molecular Regression.

- **QM7** dataset is a subset of GDB-13, which records the computed atomization energies of stable and synthetically accessible organic molecules, such as HOMO/LUMO, atomization energy, etc. It contains various of molecular structures such as triple bonds, cycles, amide, epoxy, etc [19].
- **QM8** dataset contains computer-generated quantum mechanical properties, e.g., electronic spectra and excited state energy of small molecules [20].
- **ESOL** documents the solubility of compounds [27].
- **Lipophilicity** dataset is selected from ChEMBL database, which is an important property that affects the molecular membrane permeability and solubility. The data is obtained via octanol/water distribution coefficient experiments [28].
- **FreeSolv** dataset is selected from the Free Solvation Database, which contains the hydration free energy of small molecules in water from both experiments and alchemical free energy calculations [29].

Table 1 summaries the above information, including the number of tasks and evaluation metrics of all datasets.

4.2 Baselines

We thoroughly evaluate the performance of our methods with several popular baselines from both machine learning and chemistry community. The post-fix Reg indicates the method for the regression task. Among them,

- Inuence Relevance Voting (IRV) is a KNN classifier based on the molecular fingerprints[30].
- TF_Roubust/TF_Reg [31] and LogReg [32] are two multitask model based on Deep Neural Network and Logistic Regression respectively.
- Random Forest(RF/RF_Reg) [33] is a decision tree based ensemble prediction model, each individual tree model is trained on a subset of the original dataset. The final result is generated by the ensemble of each decision tree prediction.
- GraphConv and Weave are two GNN-based model which consider the molecules as graphs.

We use the implementation of these baselines in MoleculeNet[34]. Furthermore, we report the performance of Node-MPN [15] and Edge-MPN [21] to validate the effectiveness of the dual architecture of DualMPNN.

In addition, to demonstrate the effectiveness of shared self-attentive readout and the disagreement loss in DualMPNN, we also implement two naive schemes that one concatenates the mean-pooling outputs of the two sub-models and the other one concatenates the self-attentive outputs⁴ of the two sub-models. These two schemes are denoted as Concat + Mean and Concat + Attn respectively.

⁴We do not share the attention here.

Table 2: The performance comparison of classification tasks on AUC-ROC (higher is better) based on the scaffold split.

Method	BACE	BBBP	Tox21	ToxCast	SIDER	ClinTox
IRV	0.838 \pm 0.055	0.877 \pm 0.051	0.699 \pm 0.055	0.604 \pm 0.037	0.595 \pm 0.022	0.741 \pm 0.069
TF_Robust	0.824 \pm 0.022	0.860 \pm 0.087	0.698 \pm 0.012	0.585 \pm 0.031	0.607 \pm 0.033	0.765 \pm 0.085
LogReg	0.844 \pm 0.040	0.835 \pm 0.067	0.702 \pm 0.028	0.613 \pm 0.033	0.583 \pm 0.034	0.733 \pm 0.084
RF	0.856 \pm 0.019	0.881 \pm 0.050	0.744 \pm 0.051	0.582 \pm 0.049	0.622 \pm 0.042	0.712 \pm 0.066
GraphConv	0.854 \pm 0.011	0.877 \pm 0.036	0.772 \pm 0.041	0.650 \pm 0.025	0.593 \pm 0.035	0.845 \pm 0.051
Weave	0.791 \pm 0.008	0.837 \pm 0.065	0.741 \pm 0.044	0.678 \pm 0.024	0.543 \pm 0.034	0.823 \pm 0.023
Node-MPN	0.815 \pm 0.044	0.913 \pm 0.041	0.808 \pm 0.024	0.691 \pm 0.013	0.595 \pm 0.030	0.879 \pm 0.054
Edge-MPN	0.852 \pm 0.053	0.919 \pm 0.030	0.826 \pm 0.023	0.718 \pm 0.011	0.632 \pm 0.023	0.897 \pm 0.040
Concat + Mean	0.842 \pm 0.004	0.930 \pm 0.002	0.816 \pm 0.003	0.721 \pm 0.001	0.621 \pm 0.007	0.882 \pm 0.008
Concat + Attn	0.832 \pm 0.007	0.931 \pm 0.006	0.819 \pm 0.003	0.728 \pm 0.002	0.632 \pm 0.008	0.913 \pm 0.009
DualMPNN	0.863\pm0.002	0.938\pm0.003	0.833\pm0.001	0.729\pm0.006	0.644\pm0.003	0.930\pm0.003

4.3 Experimental Configuration

Dataset Splitting. We apply the scaffold splitting for all tasks on all datasets. Random splitting is a common process to split the dataset into train, validation and test. However, it does not simulate the real-world use case for evaluating molecule-related machine learning methods[35]. **Scaffold Splitting** splits the molecules with distinct two-dimensional structural frameworks into different subsets[35], which is more meaningful and consequential for molecular property prediction. Yet, it is much more strict and difficult for the learning algorithm to accomplish satisfactory performance. To alleviate the effects of randomness and over-fitting, as well as to boost the robustness of the experiments, we apply cross-validation on all the experiments. All of our experiments run 10 randomly-seeded 8:1:1 data splits by scaffold splitting, which follows the same protocols in [21].

Evaluation All classification tasks are evaluated by AUC-ROC. For regression task, we apply MAE and RMSE to evaluate the performance of regression task on different datasets. Please refer Table 1 for details.

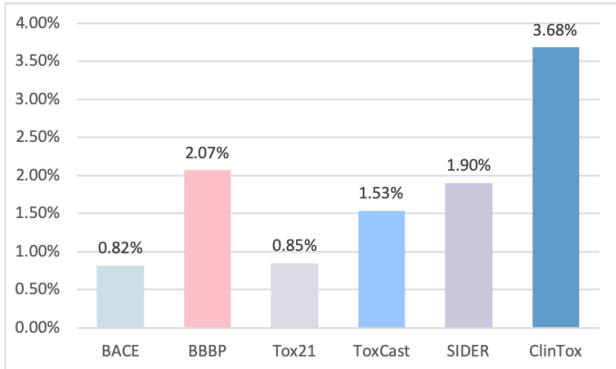


Figure 5: Improvement visualization between DualMPNN with the second-best SOTA on classification tasks.

4.4 Performance Evaluation on Classification Task

We report all the results of classification task in Table 2. To evaluate the robustness of our method, we report the mean and standard deviation of 10 times runs with different random seeds for DualMPNN and its variants. As shown in Table 2, we have these findings: (1) Clearly, our DualMPNN gains significant enhancement against SOTAs on all datasets consistently. Specifically, DualMPNN gains the average AUC boost by 1.81% on average compared with the SOTAs on each dataset, which is regarded as the remarkable boost, considering the challenges on these benchmarks. The detailed improvement visualization can be found in Figure 5. (2) Either traditional methods or graph convolutional networks do not perform well in these challenges benchmarks. This may be because that these methods fail to integrate the rich information attached on nodes/edges. (3) Compared with Node-MPN and Edge-MPN, DualMPNN has much smaller standard deviation. It indicates that DualMPNN is more robust than Node-MPN and Edge-MPN. (4) Compared with two simple variants, DualMPNN demonstrates the superiority both on performance and robustness. It validates the effectiveness of the dual path architecture with disagreement loss constraint.

4.5 Ablation Study on Model Structures

In this section, we defer more discussions regarding to the impacts of two key components in the proposed DualMPNN, the disagreement loss and the shared self-attentive readout. We report the results of three datasets to evaluate the impacts. In Table 3, the results demonstrate that the primary structure of dual training model overall performs the best on all three datasets. Moreover, we find that both attention and disagreement loss can boost the performance compared with No All. Particularly, when the self-attention mechanism is employed into the model, the performance has already surpassed all the baseline models including Node-MPN and Edge-MPN, which proves that the molecular property is affected by the various atoms differently. Hence, the weights of every atoms should not be considered equivalently. Overall, the proposed DualMPNN that adopts both disagreement loss and self-attention outperforms the other variants, indicating that the combination of them would significantly facilitate the model learning.

Table 3: Ablation Study on the variants of DualMPNN

	ToxCast	SIDER	ClinTox
No All	0.718	0.644	0.852
Only Attention	0.728	0.646	0.901
Only Disagreement Loss	0.722	0.648	0.863
DualMPNN	0.731	0.652	0.907

4.6 Additional Results on Regression Task

To evaluate the effectiveness of DualMPNN on various kinds of tasks, we report more results of DualMPNN on regression task. The performance is assessed on five benchmark datasets and five baseline models. The results are shown in Table 4. As we can see, DualMPNN achieves the best performance on regression tasks too. Specifically, our method relatively improve 24.6% over other models on QM7 dataset, yet again, reveals the superiority and robustness of DualMPNN.

Table 4: The performance comparison of regression task based on scaffold split (smaller is better). The evaluation metric of QM7/QM8 is MAE and that of ESOL/Lipo/FreeSolv is RMSE.

Method	QM7	QM8	ESOL	Lipo	FreeSolv
TF_Reg	120.562 \pm 9.600	0.024 \pm 0.001	1.722 \pm 0.038	0.909 \pm 0.060	4.122 \pm 0.085
GraphConv	118.875 \pm 20.219	0.021 \pm 0.001	1.068 \pm 0.050	0.712 \pm 0.049	2.900 \pm 0.135
Weave	94.688 \pm 2.705	0.022 \pm 0.001	1.158 \pm 0.055	0.813 \pm 0.042	2.398 \pm 0.250
NB-MPN	112.960 \pm 17.211	0.015 \pm 0.002	1.167 \pm 0.430	0.672 \pm 0.051	2.185 \pm 0.952
EB-MPN	105.775 \pm 13.202	0.0143 \pm 0.0023	0.980 \pm 0.258	0.653 \pm 0.046	2.177 \pm 0.914
DualMPNN	71.325 \pm 2.843	0.0127 \pm 0.0005	0.8049 \pm 0.036	0.599 \pm 0.016	1.840 \pm 0.194

4.7 Case Study: The Interpretability Visualization

To illustrate the interpretability of DualMPNN, we visualize certain molecules with the learned attentions of DualMPNN associated with each atom within one molecule from Clintox dataset, with toxicity as the label. Figure 6 instantiates the graph structures of the molecules along with the corresponding atom attentions. The attention values lower than 0.01 are omitted. We observe that different atoms indeed react distinctively: **1).** Most atom carbon (C) that are responsible for constructing the molecule topology have got zero attention value. It is because these kinds of sub-structures would not effect the toxicity of a compound. **2).** Beyond that, DualMPNN promotes the learning of the functional groups with impression on molecular toxicity, e.g., toxic functional group **trifluoromethyl** and **cyanide** are known for the toxicity [36], which reveal extremely high attention value in Figure 6. These high attention values can be exploited as the explanation of the toxicity of the given molecules.

Furthermore, we provide a comprehensive statistics of the attention values over the entire ClinTox dataset. Figure 7 demonstrates the average attention values for single elements, as well as the total occurrences of each element. It is notable that, **1).** atoms with high frequency do not receive high attention. For example, atom C is an essential element to maintain the molecular topology so that it does not have significant impact on the toxicity. **2).** atoms with low frequency but high attention values are generally heavy elements. For example, Hg (Mercury) is widely known by its toxicity.

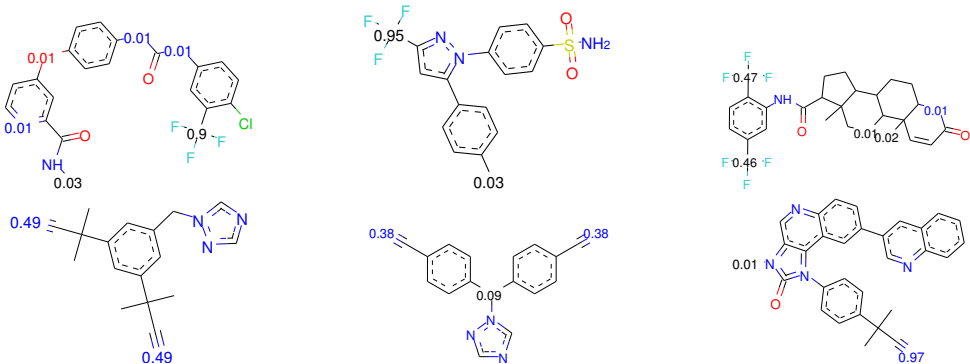


Figure 6: The visualization of attention value on molecules in ClinTox. The attention value smaller than 0.01 is omitted. Different color indicates different elements: black: C, blue: N, red: O, green: Cl, yellow: S, sky-blue: F. The former three molecules: the molecules with trifluoromethyl. The latter three molecules: the molecules with cyano.

The accompanied attention value of Hg is relevantly high because it usually affects the toxic property greatly. Both above observations yield our assumption that regarding atoms should be considered with different weights. Overall, compared with the previous models, DualMPNN is able to provide strong interpretability for the prediction results, which is crucial for the real drug discovery applications.

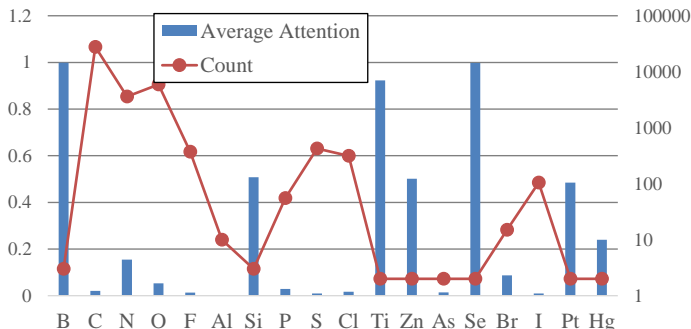


Figure 7: The statistics of attention in ClinTox. Left axis: the average attention value of the element. Right axis: the count of the element.

5 Related Work

Hand-crafted molecular fingerprints based methods. The traditional feature extraction method enlists experts to design the molecule fingerprint manually, based on biological experiments and chemical knowledge [37], such as the property of molecule sub-structures. These types of fingerprint methods generally work well for particular tasks but lack universality. Hash-based methods have been developed to address this issue by generating unique fingerprints based on the extracted molecular features. One critical approach is called circular fingerprints [1]. Circular fingerprints employ a fixed hash function to extract each layer’s features of a molecule based on the concatenated features of the neighborhood in the previous layer. Extended-Connectivity Fingerprint is one of the most famous examples of hash-based fingerprints (ECFP) [38]. Generated fingerprint representations usually go through machine learning techniques to perform further predictions, such as Logistic Regression, Random Forest, Influence Relevance Voting (IRV), and Multitask Networks. Logistic Regression predicts the binary label by learning the coefficient combination of a logistic function based on the input features [39]. Random Forest is a widely used machine learning technique for prediction [33]. The prediction result is ensemble by each individual prediction of multiple decision tree models, from which each decision tree model is trained over a subset of the original dataset. IRV assumes similar sub-structures reveal similar functionality; it predicts the test sample label by grouping the labels of top K compounds, which contain similar sub-structures [30]. A Multitask Network takes the joint molecular featurizations along all tasks as input, then feeds them into fully connected neural networks for prediction[31]. Nonetheless, this type of hand-crafted fingerprint has a very notable problem: since the characteristic of the hash function is non-invertible, it might not be able to catch enough information when converting.

SMILES sequence based techniques. SMILES sequence-based models [40] spot the potentially useful information of molecular SMILES sequence data by adequately training them using Recurrent Neural Network, in order to obtain

the vector representation of the molecule. These vectors then go through other supervised models to perform property prediction, e.g., GradientBoost [41]. The SMILES-based models are inspired by the sequence learning in Natural Language Processing [42], which takes an unlabeled dataset as input to convert a SMILES to a fingerprint, then recovers the fingerprint back to a sequence representation for better learning. The high-performance fingerprint training model could be used to generate the fingerprints for other SMILES; then the corresponding molecular fingerprint is suitable for prediction purposes.

Graph structure based techniques. The molecule could be represented as a graph based on its chemical structure, e.g., consider the atoms as the vertexes, and the bonds between the atoms as the edges. Thus, many graph theory algorithms could be applied to represent a molecule by embedding the graph features into a continuous vector [34, 43, 44]. A noted study proposed the idea of neural fingerprints, which applies convolutional networks on graphs directly [45]. The difference between Neural Fingerprint and Circular Fingerprint is the replacement of the hash function. Neural Fingerprint applies a non-linear activated densely connected layer to generate the fingerprint. This innovative Graph Convolutional Networks (GCN) [46] is inspired by deep Graph Convolutional Neural Network [45], and established by learning a function on graph node features and the graph structure matrix representation [12, 43]. Other promising graph-based models such as the Weave model have also been proposed. The weave model could be considered as a specific convolution model. The key difference is the updating procedure of the atom features. It combines all the atoms in a molecule with their matching pairs instead of the neighbors of the atoms.

6 Conclusions

We propose a comprehensive Dual Message Passing Neural Network (DualMPNN) for molecular property prediction tasks by learning molecular representation from the graph structures. Unlike previous attempts focused exclusively on either atom-oriented graph structures or bond-oriented graph structures, our method, inspired by multi-view learning, takes both atom and bond information into consideration. DualMPNN consists of two branches: the Node-central Encoder, which allows the node message to recast by the aggregation of neighbor nodes, and the Edge-central Encoder, which recasts the edge message by aggregating the neighbor edge features. According to the dual training, two graph representations are generated and fed forward respectively to a fully connected neural network to predict the property label. To assure the two models’ circulation during the training, as well as to learn the atom importance within the molecule, a self-attention mechanism is employed in the readout phase to flatten the feature matrices from the two models into two molecular vector representations. Since the two vectors are actually the expressions of the same object, a disagreement loss is introduced to restrain the distance between them. Extensive experiments on the comparison of our model with state-of-the-art techniques demonstrate that DualMPNN outperforms all the baselines significantly, as well as equips with strong robustness. In addition, the attention module brings in the interpretability of the proposed model, as well as justifies the consequence of atom importance for property prediction, which provides another promising perspective in the domain of drug discovery.

References

- [1] Robert C Glen, Andreas Bender, Catrin H Arnby, Lars Carlsson, Scott Boyer, and James Smith. Circular fingerprints: flexible molecular descriptors with applications from physical chemistry to adme. *IDrugs*, 9(3):199, 2006.
- [2] Steven M Paul, Daniel S Mytelka, Christopher T Dunwiddie, Charles C Persinger, Bernard H Munos, Stacy R Lindborg, and Aaron L Schacht. How to improve r&d productivity: the pharmaceutical industry’s grand challenge. *Nature reviews Drug discovery*, 9(3):203, 2010.
- [3] Travers Ching, Daniel S Himmelstein, Brett K Beaulieu-Jones, Alexandr A Kalinin, Brian T Do, Gregory P Way, Enrico Ferrero, Paul-Michael Agapow, Michael Zietz, Michael M Hoffman, et al. Opportunities and obstacles for deep learning in biology and medicine. *Journal of The Royal Society Interface*, 15(141):20170387, 2018.
- [4] Petar Veličković, Guillem Cucurull, Arantxa Casanova, Adriana Romero, Pietro Lio, and Yoshua Bengio. Graph attention networks. *arXiv preprint arXiv:1710.10903*, 2017.
- [5] Wenbing Huang, Tong Zhang, Yu Rong, and Junzhou Huang. Adaptive sampling towards fast graph representation learning. In *NeurIPS*, pages 4558–4567. 2018.
- [6] Kelvin Guu, John Miller, and Percy Liang. Traversing knowledge graphs in vector space. *arXiv preprint arXiv:1506.01094*, 2015.
- [7] Will Hamilton, Payal Bajaj, Marinka Zitnik, Dan Jurafsky, and Jure Leskovec. Embedding logical queries on knowledge graphs. In *Advances in Neural Information Processing Systems*, pages 2026–2037, 2018.

- [8] Mingsong Mao, Jie Lu, Guangquan Zhang, and Jinlong Zhang. Multirelational social recommendations via multigraph ranking. *IEEE transactions on cybernetics*, 47(12):4049–4061, 2016.
- [9] Federico Monti, Michael Bronstein, and Xavier Bresson. Geometric matrix completion with recurrent multi-graph neural networks. In *Advances in Neural Information Processing Systems*, pages 3697–3707, 2017.
- [10] Greeshma Neglur, Robert L Grossman, and Bing Liu. Assigning unique keys to chemical compounds for data integration: Some interesting counter examples. In *International Workshop on Data Integration in the Life Sciences*, pages 145–157. Springer, 2005.
- [11] Douglas EV Pires, Tom L Blundell, and David B Ascher. pkcsm: predicting small-molecule pharmacokinetic and toxicity properties using graph-based signatures. *Journal of medicinal chemistry*, 58(9):4066–4072, 2015.
- [12] Alex Fout, Jonathon Byrd, Basir Shariat, and Asa Ben-Hur. Protein interface prediction using graph convolutional networks. In *NeurIPS*, pages 6530–6539, 2017.
- [13] Sanjivanjit K Bhal. Logpmaking sense of the value. *Advanced Chemistry Development, Toronto, ON, Canada*, pages 1–4, 2007.
- [14] Kristina Preuer, Günter Klambauer, Friedrich Rippmann, Sepp Hochreiter, and Thomas Unterthiner. Interpretable deep learning in drug discovery. In *Explainable AI: Interpreting, Explaining and Visualizing Deep Learning*, pages 331–345. Springer, 2019.
- [15] Justin Gilmer, Samuel S Schoenholz, Patrick F Riley, Oriol Vinyals, and George E Dahl. Neural message passing for quantum chemistry. In *ICML*, pages 1263–1272. JMLR. org, 2017.
- [16] Shiliang Sun. A survey of multi-view machine learning. *Neural computing and applications*, 23(7-8):2031–2038, 2013.
- [17] Ann M Richard, Richard S Judson, Keith A Houck, Christopher M Grulke, Patra Volarath, Inthirany Thillainadara-jah, Chihae Yang, James Rathman, Matthew T Martin, John F Wambaugh, et al. Toxcast chemical landscape: paving the road to 21st century toxicology. *Chemical research in toxicology*, 29(8):1225–1251, 2016.
- [18] Ines Filipa Martins, Ana L Teixeira, Luis Pinheiro, and Andre O Falcao. A bayesian approach to in silico blood-brain barrier penetration modeling. *Journal of chemical information and modeling*, 52(6):1686–1697, 2012.
- [19] L. C. Blum and J.-L. Reymond. 970 million druglike small molecules for virtual screening in the chemical universe database GDB-13. *J. Am. Chem. Soc.*, 131:8732, 2009.
- [20] Raghunathan Ramakrishnan, Mia Hartmann, Enrico Tapavicza, and O Anatole Von Lilienfeld. Electronic spectra from tddft and machine learning in chemical space. *The Journal of chemical physics*, 143(8):084111, 2015.
- [21] Kevin Yang, Kyle Swanson, Wengong Jin, Connor Coley, Philipp Eiden, Hua Gao, Angel Guzman-Perez, Timothy Hopper, Brian Kelley, Miriam Mathea, et al. Analyzing learned molecular representations for property prediction. *Journal of chemical information and modeling*, 59(8):3370–3388, 2019.
- [22] Frank Harary and Robert Z. Norman. Some properties of line digraphs. *Rendiconti del Circolo Matematico di Palermo*, 9(2):161–168, May 1960.
- [23] Jia Li, Yu Rong, Hong Cheng, Helen Meng, Wenbing Huang, and Junzhou Huang. Semi-supervised graph classification: A hierarchical graph perspective. In *The World Wide Web Conference*, pages 972–982. ACM, 2019.
- [24] Govindan Subramanian, Bharath Ramsundar, Vijay Pande, and Rajiah Aldrin Denny. Computational modeling of β -secretase 1 (bace-1) inhibitors using ligand based approaches. *Journal of chemical information and modeling*, 56(10):1936–1949, 2016.
- [25] Michael Kuhn, Ivica Letunic, Lars Juhl Jensen, and Peer Bork. The sider database of drugs and side effects. *Nucleic acids research*, 44(D1):D1075–D1079, 2015.
- [26] Kaitlyn M Gayvert, Neel S Madhukar, and Olivier Elemento. A data-driven approach to predicting successes and failures of clinical trials. *Cell chemical biology*, 23(10):1294–1301, 2016.
- [27] John S Delaney. Esol: estimating aqueous solubility directly from molecular structure. *Journal of chemical information and computer sciences*, 44(3):1000–1005, 2004.
- [28] Anna Gaulton, Louisa J Bellis, A Patricia Bento, Jon Chambers, Mark Davies, Anne Hersey, Yvonne Light, Shaun McGlinchey, David Michalovich, Bissan Al-Lazikani, et al. ChEMBL: a large-scale bioactivity database for drug discovery. *Nucleic acids research*, 40(D1):D1100–D1107, 2011.
- [29] David L Mobley and J Peter Guthrie. Freesolv: a database of experimental and calculated hydration free energies, with input files. *Journal of computer-aided molecular design*, 28(7):711–720, 2014.

- [30] S Joshua Swamidass, Chloé-Agathe Azencott, Ting-Wan Lin, Hugo Gramajo, Shiou-Chuan Tsai, and Pierre Baldi. Influence relevance voting: an accurate and interpretable virtual high throughput screening method. *Journal of chemical information and modeling*, 49(4):756–766, 2009.
- [31] Bharath Ramsundar, Steven Kearnes, Patrick Riley, Dale Webster, David Konerding, and Vijay Pande. Massively multitask networks for drug discovery. *arXiv preprint arXiv:1502.02072*, 2015.
- [32] Jerome Friedman, Trevor Hastie, Robert Tibshirani, et al. Additive logistic regression: a statistical view of boosting (with discussion and a rejoinder by the authors). *The annals of statistics*, 28(2):337–407, 2000.
- [33] Leo Breiman. Random forests. *Machine learning*, 45(1):5–32, 2001.
- [34] Zhenqin Wu, Bharath Ramsundar, Evan N Feinberg, Joseph Gomes, Caleb Geniesse, Aneesh S Pappu, Karl Leswing, and Vijay Pande. Moleculenet: a benchmark for molecular machine learning. *Chemical Science*, 9(2):513–530, 2018.
- [35] Guy W Bemis and Mark A Murcko. The properties of known drugs. 1. molecular frameworks. *Journal of medicinal chemistry*, 39(15):2887–2893, 1996.
- [36] J Saarikoski and M Viluksela. Influence of ph on the toxicity of substituted phenols to fish. *Archives of environmental contamination and toxicology*, 10(6):747–753, 1981.
- [37] HL Morgan. The generation of a unique machine description for chemical structures-a technique developed at chemical abstracts service. *J. Chemical Documentation*, 5:107–113, 1965.
- [38] David Rogers and Mathew Hahn. Extended-connectivity fingerprints. *Journal of chemical information and modeling*, 50(5):742–754, 2010.
- [39] David G Kleinbaum, K Dietz, M Gail, Mitchel Klein, and Mitchell Klein. *Logistic regression*. Springer, 2002.
- [40] Zheng Xu, Sheng Wang, Feiyun Zhu, and Junzhou Huang. Seq2seq fingerprint: An unsupervised deep molecular embedding for drug discovery. In *BCB*, 2017.
- [41] Jerome H Friedman. Greedy function approximation: a gradient boosting machine. *Annals of statistics*, pages 1189–1232, 2001.
- [42] Antoine Bordes, Xavier Glorot, Jason Weston, and Yoshua Bengio. Joint learning of words and meaning representations for open-text semantic parsing. In *Artificial Intelligence and Statistics*, pages 127–135, 2012.
- [43] Ruoyu Li, Sheng Wang, Feiyun Zhu, and Junzhou Huang. Adaptive graph convolutional neural networks. In *AAAI*, 2018.
- [44] Chao Shang, Qinqing Liu, Ko-Shin Chen, Jiangwen Sun, Jin Lu, Jinfeng Yi, and Jinbo Bi. Edge attention-based multi-relational graph convolutional networks. *arXiv preprint arXiv:1802.04944*, 2018.
- [45] David K Duvenaud, Dougal Maclaurin, Jorge Iparraguirre, Rafael Bombarell, Timothy Hirzel, Alán Aspuru-Guzik, and Ryan P Adams. Convolutional networks on graphs for learning molecular fingerprints. In *NeurIPS*, pages 2224–2232, 2015.
- [46] Thomas N Kipf and Max Welling. Semi-supervised classification with graph convolutional networks. *arXiv preprint arXiv:1609.02907*, 2016.
- [47] Greg Landrum et al. Rdkit: Open-source cheminformatics, 2006.
- [48] Ashish Vaswani, Noam Shazeer, Niki Parmar, Jakob Uszkoreit, Llion Jones, Aidan N Gomez, Łukasz Kaiser, and Illia Polosukhin. Attention is all you need. In *Advances in neural information processing systems*, pages 5998–6008, 2017.
- [49] Yu Rong, Wenbing Huang, Tingyang Xu, and Junzhou Huang. Dropedge: Towards deep graph convolutional networks on node classification. In *International Conference on Learning Representations*, 2020.

A The node / edge feature extraction of the molecules

The node / edge feature extraction contains two parts: 1) **node/edge messages**, which are constructed by aggregating neighbor nodes / edges features iteratively; 2) **RDKit features**, which is the additional molecule-level features generated by RDKit to capture the global molecular features. It consists of 200 features for each molecule [47]. Since we focus on the model architecture part, we follow the exact same protocol of DMPNN for the initial node(atom) and edge(bond) features selection, as well as the 200 RDKit features generation[21] procedure. The atom features description and size are listed in Table5, and the bond features are introduced in Table6. The RDKit features are concatenated with the node / edge embedding, to go through fully connected layers for the prediction tasks. All these features are obtained via RDKit[47].

Table 5: Atom Features

features	size	description
atom type	100	type of atom (ex. C, N, O), by atomic number
formal charge	5	integer electronic charge assigned to atom
number of Bonds	6	number of bonds the atom is involved in
chirality	5	number of bonded hydrogen atoms
number of H	5	number of bonded hydrogen atoms
atomic mass	1	mass of the atom, divided by 100
aromaticity	1	whether this atom is part of an aromatic system
hybridization	5	sp, sp2, sp3, sp3d, or sp3d2

Table 6: Bond Features

features	size	description
bond type	4	single, double, triple, or aromatic
stereo	6	none, any, E/Z or cis/trans
in ring	1	whether the bond is part of a ring
conjugated	1	whether the bond is conjugated

B Experiments setup and additional results

B.1 Hyper-parameter Optimization

We adopt Adam optimizer for model training. We use the Noam learning rate scheduler with two linear increase warm-up epochs and exponential decay afterwards[48].

For DualMPNN on each dataset, we try 200 different hyper-parameter combinations via random search, and take the hyper-parameter set with the best test score. To remove randomness, we conduct the experiments 10 times with different seeds, along with the best-parameter set, to get the final result. The details of the hyper-parameters of the implementation of DualMPNN is introduced in Table 8.

Table 7: The ablation study results of regression task on scaffold split (smaller is better). The evaluation metric of QM7/QM8 is MAE and that of ESOL/Lipo/FreeSolv is RMSE.

Method	QM7	QM8	ESOL	Lipo	FreeSolv
Concat + Mean	72.532 \pm 2.657	0.0129 \pm 0.0005	0.806 \pm 0.040	0.610 \pm 0.024	2.003 \pm 0.317
Concat + Attn	73.132 \pm 3.845	0.0128 \pm 0.0005	0.809 \pm 0.043	0.601 \pm 0.015	2.026 \pm 0.227
DualMPNN	71.325 \pm 2.843	0.0127 \pm 0.0005	0.8049 \pm 0.036	0.599 \pm 0.016	1.840 \pm 0.194

Table 8: Hyper-parameter Description.

Hyper-parameter	Description	Range
init_lr	initial learning rate of Adam optimizer and Noam learning rate scheduler	0.0001~0.0004
depth	number of the message passing steps (L)	2~6
hidden_size	number of the hidden dimensionality of the message passing network in two encoders (d_{hid})	7~19
dropout	dropout rate	0.5
weight_decay	weight decay percentage for Adam optimizer	0.00000001~0.000001
ffn_num_layers	number of the fully connected layers	2~4
ffn_hidden_size	number of the hidden dimensionality in the fully connected layers	7~19
bond_drop_rate [49]	random remove certain percent of edges	0~0.6
attn_hidden	number of hidden dimensionality in the self-attentive readout (d_{attn})	32~256
attn_out	number of output dimensionality in the self-attentive readout (r)	1~8
dist_coff	the coefficient of the disagreement loss (λ)	0.01~0.2

B.2 Additional results of regression tasks

Table 7 shows the results of two variants: Concat + Mean and Concat + Attn on regression datasets. The results also proves the effectiveness of DualMPNN.

Figure 8 illustrates the relative improvement from our model with other SOTAs, according to Table 4. As shown in Figure 8, DualMPNN achieves average 15.5% improvement on 5 regression benchmark datasets.

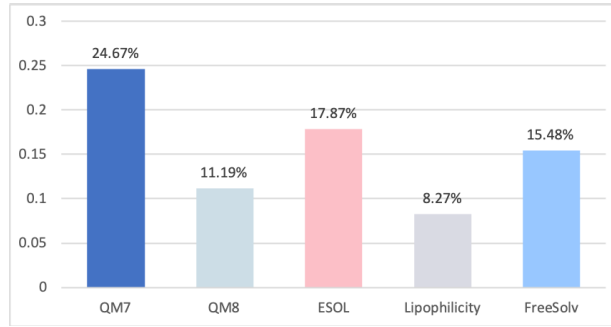


Figure 8: Improvement visualization between DualMPNN with the second-best SOTA on regression tasks.